




Article

Tool Wear and Surface Integrity of γ -TiAl Cryogenic Coolant Machining at Various Cutting Speed Levels

Xiangyu Wang ¹, Xiaoxia Zhang ¹, Duo Pan ², Jintao Niu ¹, Xiuli Fu ¹ and Yang Qiao ^{1,*}

¹ School of Mechanical Engineering, University of Jinan, Jinan 250022, China; me_wangxy@ujn.edu.cn (X.W.); 17663751979@163.com (X.Z.); me_niujt@ujn.edu.cn (J.N.); me_fuxl@ujn.edu.cn (X.F.)

² Jigang International Engineering & Technology Co., Ltd., Jinan 250098, China; me_pand@163.com

* Correspondence: me_qiaoy@ujn.edu.cn

Abstract: High-speed machining of γ -TiAl alloy is a significant challenge due to high cutting temperatures. From the perspective of environmental protection and improving tool life, appropriate cooling strategies should be adopted. Compared with dry and conventional flood cooling conditions, the feasibility of machining γ -TiAl in cryogenic LN₂ cooling conditions was discussed. The cutting force, tool wear and its mechanism, and surface roughness, as well as sub-surface morphology characteristics, were studied by combining macro and micro techniques. The results revealed that the wear morphology of the rake and flank face under the three cooling media shows different degrees. The crater wear of the rake face is expanded at high speeds and then progresses into more severe flaking and notching wear. The main wear pattern on the flank face is gradually transformed from adhesive wear to diffusion and oxidation wear at high speeds in dry machining. In the LN₂ condition, the diffusion of workpiece elements and cutting-edge oxidation were restrained. The wear pattern is still mainly adhesive wear. In addition, cryogenic machining shows significant advantages in reducing cutting force, suppressing heat-affected zone, improving surface quality, and inhibiting micro-lamellar deformation.

Keywords: cryogenic cooling; γ -TiAl alloy; high-speed machining; tool wear; surface integrity



Citation: Wang, X.; Zhang, X.; Pan, D.; Niu, J.; Fu, X.; Qiao, Y. Tool Wear and Surface Integrity of γ -TiAl Cryogenic Coolant Machining at Various Cutting Speed Levels.

Lubricants **2023**, *11*, 238. <https://doi.org/10.3390/lubricants11060238>

Received: 5 May 2023

Revised: 24 May 2023

Accepted: 25 May 2023

Published: 27 May 2023



Copyright: © 2023 by the authors. Licensee MDPI, Basel, Switzerland. This article is an open access article distributed under the terms and conditions of the Creative Commons Attribution (CC BY) license (<https://creativecommons.org/licenses/by/4.0/>).

1. Introduction

Gamma titanium aluminides (γ -TiAl) alloys are titanium aluminides with an Al content of 42–49 at.%. γ -TiAl alloys exhibit low density ($\sim 4 \text{ g}\cdot\text{cm}^{-3}$), high service temperature (650–850 °C), high specific strength, excellent creep, oxidation resistance, and [1] corrosion resistance, which makes it suitable for extreme conditions [2]. Due to remarkable advantages, γ -TiAl alloys have been commercially utilized in aero engines to partially replace Ni-based superalloys in the temperature range of 600–800 °C [3]. At present, γ -TiAl alloy has been used in engine parts such as compressor blades, turbine blades, and turbochargers [4].

However, In the cutting process, the machinability of γ -TiAl alloy is affected by its physical and chemical properties [2]. The disadvantages are as follows: the low ductility and low thermal conductivity at room temperature, resulting in surface cracks easily produced in cutting; the high hardness, strength, and work-hardening tendency, which increases the difficulty of subsequent machining. In addition, it has been pointed out in the literature [5,6] that γ -TiAl alloy has a strong chemical affinity with tool materials at high temperatures, which accelerates the deterioration of tools. Based on the above limitations, Beranoagirre et al. [7] studied the influence of different cutting parameters on tool wear in the turning test of γ -Ti Al alloy. The research results have shown that cutting speed is the main factor affecting tool life. Beranoagirre et al. [8] believed that cutting speed is the factor with maximum influence on tool life due to the growing wear originating from friction along all milling. Starting from a cutting speed of 60 m/min, a small increase of this speed,

around 15%, decreases tool life in half. The most interesting cutting speed is 50 m/min because a double machining time implies only a reduction of 15% in productivity. The surface finishes of gamma titanium–aluminum alloys in grinding are related directly to the feed rate. The surfaces obtained at low feed rates are better [9]. Some researchers [10,11] propose that the optimal cutting speed range of this alloy in conventional dry machining is that the cutting speed does not exceed 50 m/min.

Compared with conventional cutting, the advantages of high-speed cutting are not only reflected in machining efficiency but also in machining accuracy and surface finish [12]. However, it is more challenging to apply high-speed cutting technology to γ -TiAl alloys. Aspinwall et al. [13] analyzed the cutting temperature during milling γ -TiAl alloy. The cutting speed was increased from 50 to 135 m/min, resulting in a 43–47% rise in cutting temperature. Klocke et al. [14] noted that the rise of the cutting temperature caused by high speeds could soften the material. High-quality surfaces without cracks were obtained and thus improved the machinability of the difficult-to-be-machined alloy. However, this machining strategy also aggravated the negative effects of mechanical and thermal loads on the tool life, especially in dry machining. Saketi et al. [15] proposed that the rake and flank wear were the main wear pattern in TC4 low-speed cutting. Rajashree et al. [16] proposed that tool failure accelerates due to rubbing of the flank surface caused by heat and friction, reducing tool life and surface quality. The wear mechanism at high temperatures would be changed to diffusion wear. The performance of the tool deteriorated due to diffusion wear in high-speed machining. Studies have shown that similar tool wear patterns occur in γ -TiAl alloy machining [17,18].

In the above studies, the high cutting temperature is a dominant factor affecting machinability. Appropriate cooling strategies should be adopted. A reliable condition for the possibility of increasing machinability and, in turn, improved cutting conditions is the use of cooling techniques [19]. Machining of titanium alloys and its alloys is accompanied by oxidation of the chips and the machined surface [20]. Therefore, cutting fluids used in the processing of such materials should protect the chips and the treated surfaces from oxidation [21].

Cutting fluid cooling and lubrication can effectively increase tool life. González et al. [22] used Cryo CO₂ and minimal quantity lubrication (MQL) for milling the sides of Ti6Al4V integral blade rotors (IBRs). The results showed that Cryo CO₂ machining reduced the tool temperature and improved the surface quality and that the use of low-temperature lubrication reduced the amount of lubricant used and reduced production costs. Khanna et al. [23] conducted a life cycle assessment (LCA) to evaluate the environmental impact of different cutting fluid strategies throughout the entire product life cycle. The authors suggest that minimum quantity lubrication (MQL) may be a more sustainable option that still provides adequate tool life and dimensional accuracy while reducing overall environmental impact. However, the existing literature [24,25] shows that conventional flood cooling does not have obvious advantages in high-speed machining of difficult machining materials. For one thing, it is hard for the coolant to permeate through the cutting zone owing to the influence of the chip and high spindle speed. For another, the high cutting heat generated in the cutting process will make the cutting fluid evaporate rapidly, resulting in an insignificant cooling effect. In addition, the traditional cutting fluid will harm human health and the environment. Cutting fluids' airborne particles negatively affect a number of chronic human health conditions, including asthma, allergic reactions, skin rashes, and dermatological issues [16].

Cryogenic cooling is an environmentally-friendly cooling strategy which is that the conventional cutting fluid is replaced by liquid gas [26]. Cryogenic fluids are non-toxic and do not generate harmful fumes or vapors, making them an ideal choice for machining operations where people's safety is a concern [27]. According to a report from the National Institute of Standards and Technology, a cryogenic temperature is one that is lower than $-180\text{ }^{\circ}\text{C}$ [28]. Shah et al. [29] confirmed that cryogenic CO₂ and liquid nitrogen (LN₂) is suitable coolants for difficult-to-be-machined materials from energy consumption, tool life,

and surface integrity. The low-temperature LN_2 commonly used in machining applications is -196°C , and the LCO_2 is -56.6°C [16]. Khanna et al. [23] compared LCO_2 , MQL, and cryogenic machining based on machinability metrics such as cutting forces, tool wear, and surface roughness. The results showed that a higher cutting force was observed for MQL machining, followed by flood and cryogenic machining using LCO_2 in decreasing order, respectively. LCO_2 has excellent heat absorption capability due to its low boiling point (-78.5°C), a feature that allows it to effectively control tool wear. The lower tool life under MQL machining is due to its inability to extract heat, resulting in higher tool wear.

Some researchers have summarized the effect of cryogenic cooling on the tool life and surface quality of various materials, such as Ni-based superalloys [30,31], Ti-based alloys [32–34], and Iron-based alloys [35]. Its advantage is to keep the cutting temperature down and improve the heat dissipation from the cutting zone, leading to mechanical property improving and residual stress, surface roughness, and tool wear decreasing.

However, cryogenic machining has not been widely studied in view of the poor plasticity of γ -TiAl alloy at low temperatures. Klocke et al. [21] believed that cryogenic machining was a promising strategy for cutting γ -TiAl alloy, which can improve the wear resistance of tools and reduce the microstructure changes of the surface layer. Pereira et al. [36] focused on the Inconel 718 and how the internal cryo lubrication approach could improve its milling process. The researchers conducted experiments to compare this method with traditional flood cooling and found that the cryo lubrication approach resulted in lower temperatures at the cutting edge and improved tool life. They also noted that the use of a special type of coolant called a cryogenic coolant, was necessary for achieving optimal results. Priarone et al. [37] proposed that the tool wear patterns in cryogenic machining were also rake, flank, and adhesion wear. However, the influence on the wear mechanism has not been analyzed in these papers. The above studies mostly describe the positive role of the cryogenic environment in tool life and surface integrity from a macro perspective, and most of the related wear mechanism studies are based on indirect observations.

The purpose of the work is to compare and discuss the effect of dry machining, conventional flood cooling machining, and cryogenic machining on the machinability in γ -TiAl alloy high-speed cutting. The tool wear and mechanism, the cutting force, as well as its relationship with surface roughness and microstructure morphology, are studied using macro and micro technologies through turning tests at various cutting speeds.

2. Experimental Preparation

2.1. Workpiece Materials

The material was a Ti-47.5Al-2.5V-1.0Cr at% γ -TiAl alloy. The microstructure of the material after heat treatment was the $\gamma + \alpha_2$ fully lamellar structure in Figure 1. The rod workpieces were made by casting with a dimension of $\phi 110$ mm. Its mechanical properties are presented at different temperatures in Table 1.

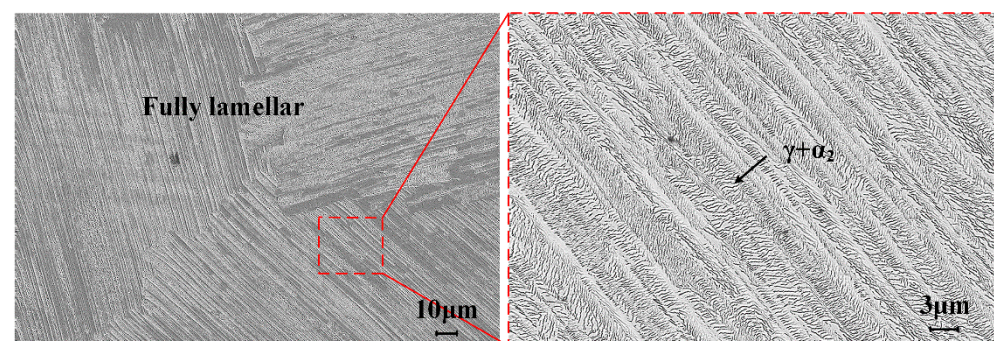


Figure 1. The SEM microstructure image of γ -TiAl alloy.

Table 1. The mechanical properties of workpiece material [18,38].

Properties	Temperature (°C)	
	25	800
Elastic modulus (GPa)	172	151
Tensile strength (GPa)	540	500
Yield strength (MPa)	440	380
Thermal conductivity (W/m·k)	18.6	23.1
Ductility (%)	1.5	6

2.2. Experimental Conditions and Processes

Face-turning tests were performed on a CNC lathe with a rated spindle speed of 4000 rpm. The uncoated carbide cutting inserts used were TPGN220408 K313 (Kennametal Inc., Pittsburgh, PA, USA). The main variables were cooling media and cutting speeds at the same cutting time. The surface roughness was measured using Surface Roughness Tester-SJ410 (MITUTOYO, Kanagawa, Japan). This device has a maximum measurement range of 800 μm ($\pm 400 \mu\text{m}$) for the calculation of various roughness parameters. The surface force was measured using YDC-III 89A piezoelectric turning dynamometer (Dalian University of Technology, Dalian, China). The measuring force range should be $< \pm 2000 \text{ N}$ in the three directions of X, Y, and Z. The experiment process parameters are displayed in Table 2.

Table 2. The experiment process parameters.

Item	Value
Cooling media	Dry, Emulsion, LN_2
Cutting speed (v_c)	60, 90, 120, 150, 180, 210 m/min
Feed rate (f)	0.1 mm/r
Cutting depth (a_p)	0.2 mm
Rake angle (γ)	3°
Relief angle (α)	8°

The cutting time is 1 min, and the effective machining length differs at different cutting speeds. Considering the poor machinability of the materials, the cutting speed of 210 m/min was not conducted in dry machining. The emulsion with a mixture ratio of 6% was selected as the conventional coolant. LN_2 was selected as the cryogenic coolant. The outlet pressure of the LN_2 tank was stabilized at 1.5 MPa during the operation. According to the test requirements, LN_2 and emulsion were respectively sprayed into the contact area of tool-workpieces. The schematic overview of the experimental setup is shown in Figure 2.

The influence of mechanical load on tool wear and surface integrity is studied by analyzing the variation of cutting force (F). The F was measured in three directions, that is, tangential force (F_x), radial force (F_y), and axial force (F_z).

After one minute of machining, the tool wear and failure morphology of the rake face and the flank face were observed by the ultra-depth of field microscope. The maximum flank wear (V_{max}) near the tool point was measured. The wear mechanism of the worn tools under three cooling media was analyzed, respectively, and cutting speeds at 60, 120, and 180 m/min were selected. The 9wear morphology was further observed by Scanning Electron Microscope (SEM) (Carl Zeiss AG, Oberkochen, Baden-Württemberg, Germany). To investigate the wear patterns, the mass fraction of the main elements in a certain wear area was obtained by Energy Dispersive Spectrometer (EDS) (Shimadzu Corporation, Kyoto, Japan).

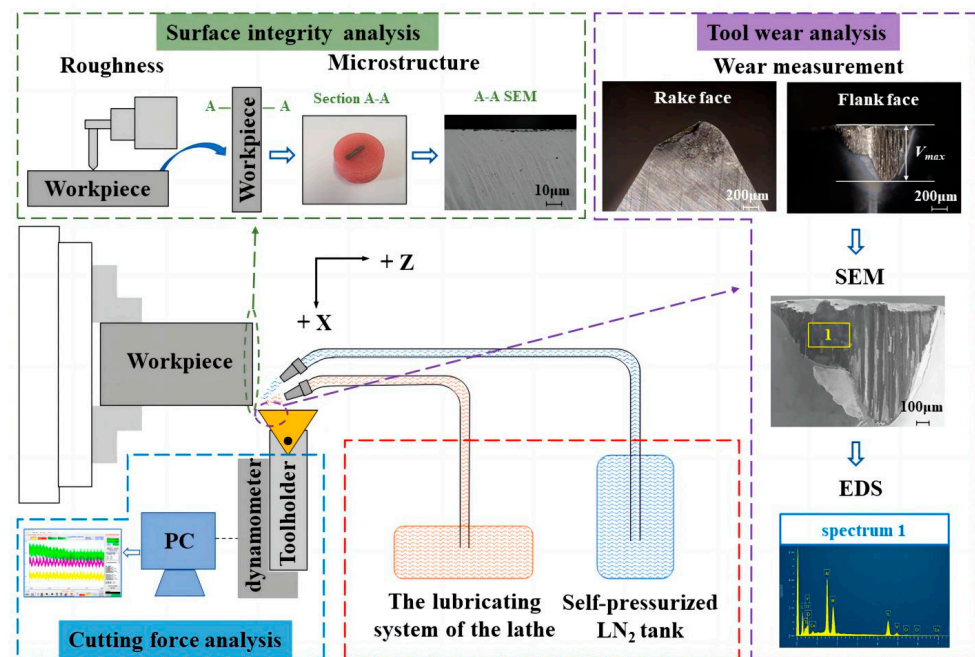


Figure 2. The experimental setup and procedure.

The related tests of surface integrity were carried out after ultrasonic cleaning for 5 min. To reduce the measurement error during the surface roughness (R_a), five different positions of each machined surface were measured along the feed direction, and the average values were calculated. To explore the deformation of the workpiece material, the cross-section was intercepted along the cutting speed direction by Wire Electrical Discharge Machining (WEDM) and then ground, polished, and cold-mounted. The cross-section was corroded with a Kroll reagent (ratio: 3% HF, 6% HNO₃, 91% distilled water) for 10 s, and the microstructure was observed by SEM.

3. Results and Discussion

3.1. Cutting Force

The variation of mechanical load at various cutting speeds and cooling conditions is analyzed in this part. The cutting force (F) is calculated by Equation (1) [39]. The variation of cutting force at various cutting speeds and cooling media is shown in Figure 3.

$$F = \sqrt{F_x^2 + F_y^2 + F_z^2} \quad (1)$$

As shown in Figure 3, the variation curve of cutting force shows an increase–decrease–increase trend along increasing cutting speeds. The cutting force under dry machining is the largest. With the increase of the cutting speed (lower than 120 m/min), the strain and strain rate of the cutting zone increase. In this case, the strain-strengthening effect is higher than the thermal softening. The degree of work hardening of the workpiece is enhanced, thereby increasing the cutting force. The value of F under the emulsion condition is almost the same as that under the LN₂ condition at low speeds, indicating that the cooling effect of emulsion and LN₂ is adequate to restrict the plastic deformation. In fact, the lubrication effect of emulsion in low-speed cutting is better than that of cryogenic cooling.

When the cutting speed is increased to a certain value, the cutting force is decreased. For example, the critical cutting speed is 120 m/min in dry cutting. The softening effect caused by the high temperature on the material increases gradually, resulting in a decrease in the strengthening. Given the cooling effect of coolants, the cutting force under emulsion cooling and cryogenic cooling decreases significantly at $v_c = 150$ m/min. Under higher speeds, the thermal softening effect tends to be stable. The work hardening trend increases continuously until it is higher than the softening again. The cutting force appears to have a

certain degree of recovery. The cutting force under the LN₂ condition is relatively small in the higher speed range because its sufficient cooling effect can suppress plastic deformation.

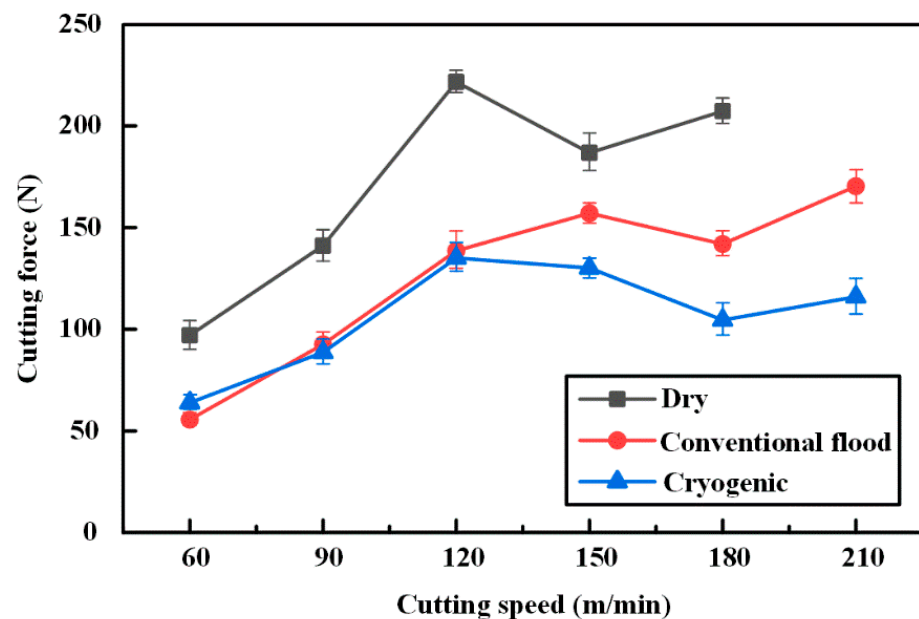


Figure 3. The cutting force under various conditions.

3.2. Tool Wear

Tool wear as a criterion to judge the machinability of materials is affected by tool material, cutting parameters, and cooling conditions. The effect of coolant on tool wear at various cutting speeds is evaluated in this part.

The maximum flank wear (V_{max}) and its morphology near the tool point under various cutting conditions are shown in Figure 4. The trends indicated that the wear degree is almost positively correlated with the cutting speeds, which is the same as the variation of the F .

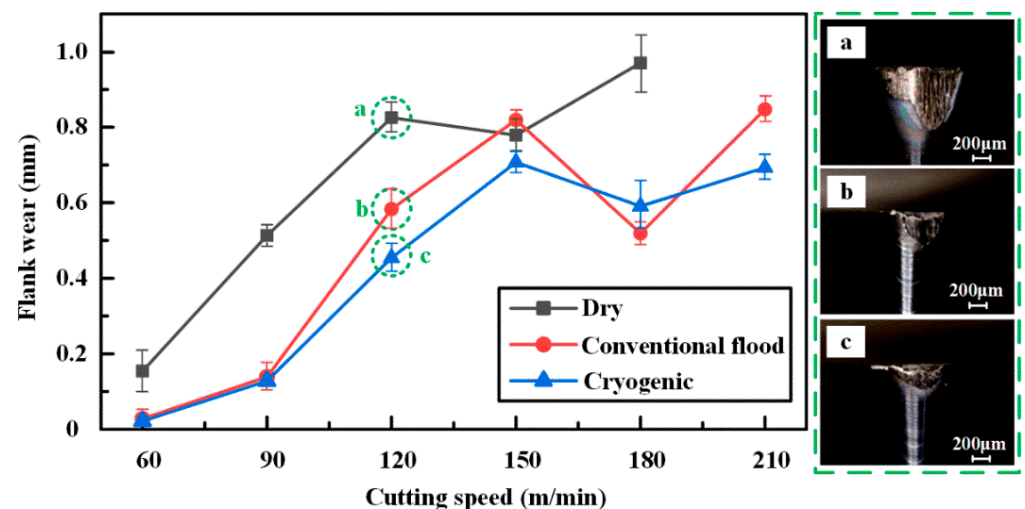


Figure 4. The maximum flank wear near the tool point and its morphology. (a) Dry cutting at $v_c = 120$ m/min, (b) Cutting under conventional flood at $v_c = 120$ m/min, (c) Cutting under cryogenic at $v_c = 120$ m/min.

According to the tool wear morphology under three cooling conditions, the flank wear is the most serious in dry machining at $v_c = 120$ m/min. This is due to the most violent friction between the machining surface and the tool flank face caused by the largest cutting force under dry machining. Yuan et al. [38] proposed that during the cutting process,

severe friction occurs between the chip and the rake face, the workpiece, and the flank face, resulting in the high contact pressure and temperature. The workpiece material is easily bonded to the tool under high temperatures and high pressure. Part of the binder and the tool surface material is taken away by the flowing chip and the rotating workpiece, resulting in tool bonding wear, which is similar to the conclusions of this study. In addition, the flank wear is also affected by the elastic modulus of the workpiece material [40]. The temperature in the cutting zone increases in dry machining, which reduces the elastic modulus and further increases the resilience of the machining surface. The contact area of the tool flank face and the machined surface is expanded, increasing the wear area. The intervention of emulsion and LN_2 alleviate the impact of high temperature on tool life and change the friction characteristics of the tools and chips, which improves the performance of the tool. Therefore, the tool wear in conventional flood cooling and the cryogenic condition is significantly lower than that under dry conditions.

The tool wear degree decreases to a certain extent in dry machining at $v_c = 150$ m/min. Similarly, the decrease occurs under the other two conditions, but to different degrees and at $v_c = 180$ m/min. It is preliminarily considered that the cutting layer metal is softened at high temperatures. The hardness of the material and the cutting force is decreased, thus reducing the tool wear. The cooling effect of emulsion and LN_2 weakens the thermal softening effect compared to dry machining. Therefore, the tool wear curve turns at higher cutting speeds.

When $v_c = 180$ m/min, the flank wear under the cryogenic condition is slightly higher than that under the emulsion condition. Combined with the rake wear morphology in Figure 5, the flaking wear is observed. This may be due to tool embrittlement in the extremely low environment. As a result, the flaking wear greatly reduces the tool's strength. However, the overall trend shows that LN_2 -assisted cutting has a significant advantage over the other two conditions in reducing tool wear at both low and high speeds.

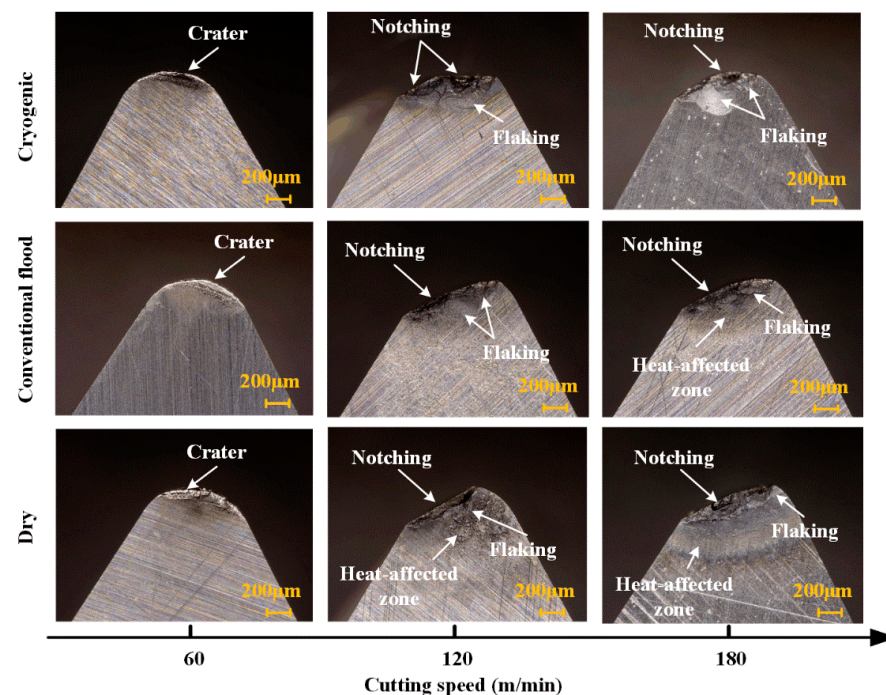


Figure 5. The rake wear morphology.

Under three cooling conditions, the crater wear is also observed in Figure 5 at $v_c = 60$ m/min. The crater is progressed into more severe flaking and notching wear at high speeds. The tool is seriously damaged at $v_c = 180$ m/min in dry machining. It can also be observed that the size of a heat-affected zone on the rake face is different in the various tools. This is the result of a large amount of cutting heat in the material removal.

The oxidation reaction occurs on the tool surface under a high-temperature environment. Comparing the morphology of the rake face under the three conditions, it can be concluded that the cryogenic condition is helpful in inhibiting the wear expansion of the crater wear and reduce the heat-affected area.

3.3. Wear Mechanism

The flank wear morphology and EDS analysis under various conditions are characterized in Figures 6–8. The obvious scratches on the tool flank face are found in the SEM morphology images. For one thing, the hard particles in the workpiece scratch the flank face in machining, resulting in abrasive wear. For another, it is clear in Figure 9 that the tool material flakes off and could stick to the flank face in a high-temperature environment. The friction between the adhered tool material and the workpiece could cause scratches. The involvement of emulsion and LN_2 achieves better friction characteristics, and their cooling capacity can help to keep the hardness of the tool, resulting in less significant scratches and wear, as shown in Figures 7 and 8.

It can be seen in Figures 6–8 that the elements of workpiece material appear on the worn tool, such as Ti and Al. However, few W elements are detected. In particular, no Co element is detected at $v_c = 60$ m/min. It is indicated that almost the whole wear area has been covered by the workpiece material. Moreover, this phenomenon occurs in all three cutting conditions. The strong chemical affinity between γ -TiAl alloy and cemented carbide tools and the high cutting temperature are the main reasons. Under the high temperature and pressure environment, the friction resistance of chip outflow increases, and an adhesive or chip retention layer is formed on the tool surface. Since the maximum probe depth of the EDS probe is $1\text{ }\mu\text{m}$, the thickness of the adhesion should be more than $1\text{ }\mu\text{m}$. As shown in Figure 10, the adhesive layer at the wear boundary falls off. The adhered materials are pulled by the flowing chips and rotating workpieces, resulting in adhesive wear.

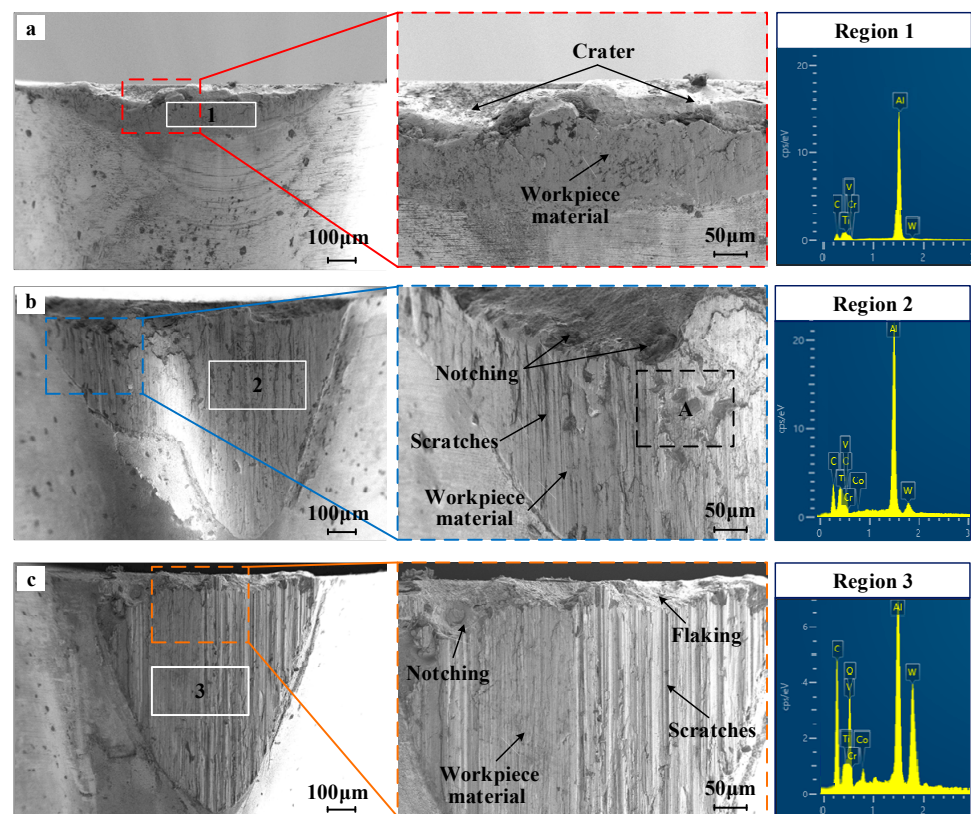


Figure 6. The flank wear morphology and EDS analysis under dry conditions. (a) $v_c = 60$ m/min; (b) $v_c = 120$ m/min; (c) $v_c = 180$ m/min.

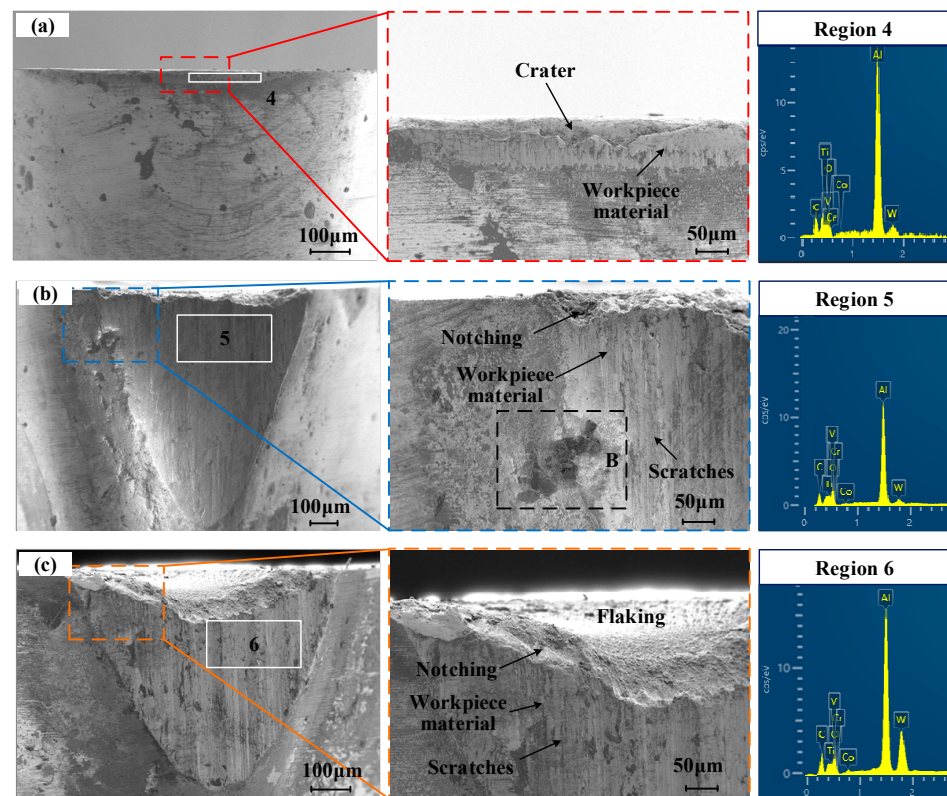


Figure 7. The flank wear morphology and EDS analysis under conventional flood cooling conditions. (a) $v_c = 60$ m/min; (b) $v_c = 120$ m/min; (c) $v_c = 180$ m/min.

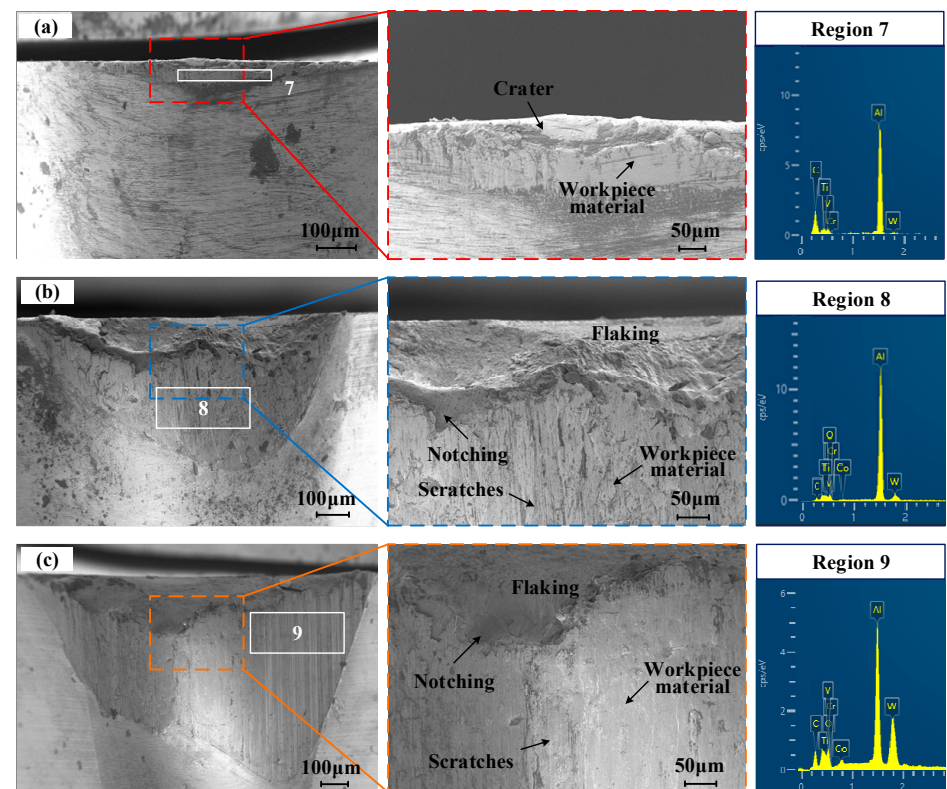


Figure 8. The flank wear morphology and EDS analysis under cryogenic cooling condition (a) $v_c = 60$ m/min; (b) $v_c = 120$ m/min; (c) $v_c = 180$ m/min.

By comparing the variations of element composition on the worn tool surface, as shown in Tables 3–5, it can be found that the fraction of C and O increases at high speeds overall. One reason is that the carbide in the tool is relatively more stable at high temperatures, increasing the mass fraction of C retained. The other is that the tool material has an oxidation reaction with oxygen in the air, affected by the high-temperature environment. Under the emulsion and LN₂-assisted cooling conditions, there are few O and C in the wear area. Klocke et al. [21] analyzed the effects of different cooling options (dry, overflow, high pressure, MQL, and cryogenic) on turning Gamma TiAl alloy. It has been proven that low-temperature cooling is the most effective lubrication strategy for this material. Compared with traditional lubrication, liquid nitrogen can reduce flank wear by up to 61%, which is similar to the conclusions of this study. The oxidation and diffusion can be alleviated at low temperatures. This advantage is more significant in the LN₂ conditions. Meanwhile, due to diffusion wear, elements such as Co, C, and W in the carbide tool will diffuse when the cutting temperature increases. Due to the diffusion of Co, carbide will reduce its bonding strength to the substrate due to the reduction of the binder Co, which will accelerate the wear of the tool. The metal and carbon atoms in the tool diffuse into the workpiece material bonded to the tool surface and are carried away by the chips. In addition, the mass fraction of Ti and Al decreases at high cutting speeds while the mass fraction of W increases greatly, which shows that the plasticity of the material has increased and the tool adhesion phenomenon is reduced. The degree of adhesion is negatively correlated with the cutting speed. It is also noted from Figures 6–8 that the adhesion phenomenon is the most serious in dry conditions, followed by conventional flood cooling and cryogenic conditions. The main reason is that the coolant has an inhibitory effect on the chemical activity of the workpiece material. Especially under the LN₂ conditions, the tool adhesion has been effectively suppressed with an outstanding cooling effect. However, the mass fraction of elements such as Ti, Al, and V is still higher than that of W at high speeds in LN₂ conditions, which indicates that the adhesion phenomenon is still serious. The wear pattern is still dominated by adhesive wear during high-speed cutting.

Table 3. The element composition of region 1/2/3.

Cutting Speed	Element Composition (at%)							
	Ti	Al	V	Cr	W	C	Co	O
60	30.45	40.66	1.04	4.15	0.17	23.65	-	-
120	21.88	29.89	0.27	2.36	0.10	25.49	0.47	19.53
180	17.56	28.81	0.68	1.51	0.25	29.38	0.55	21.26

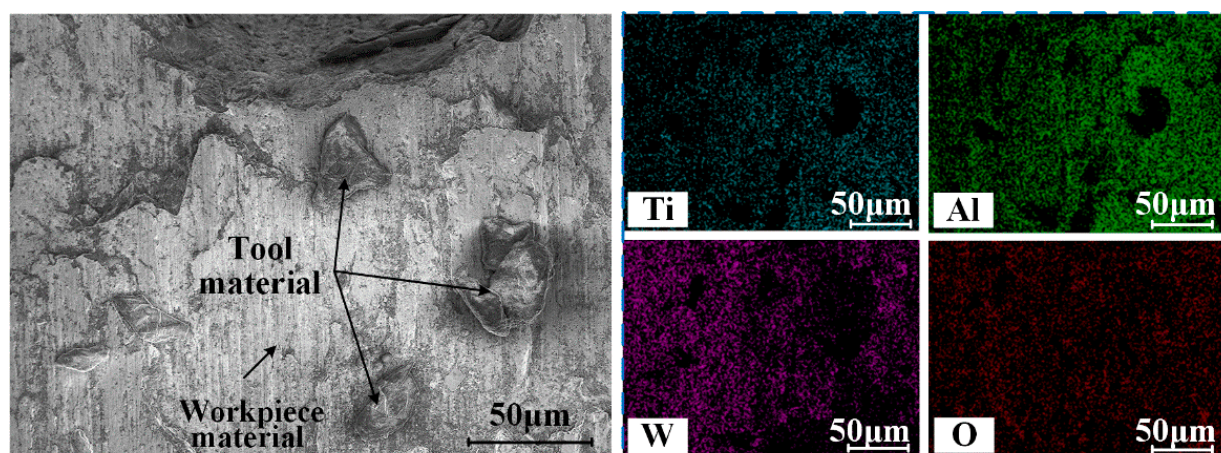
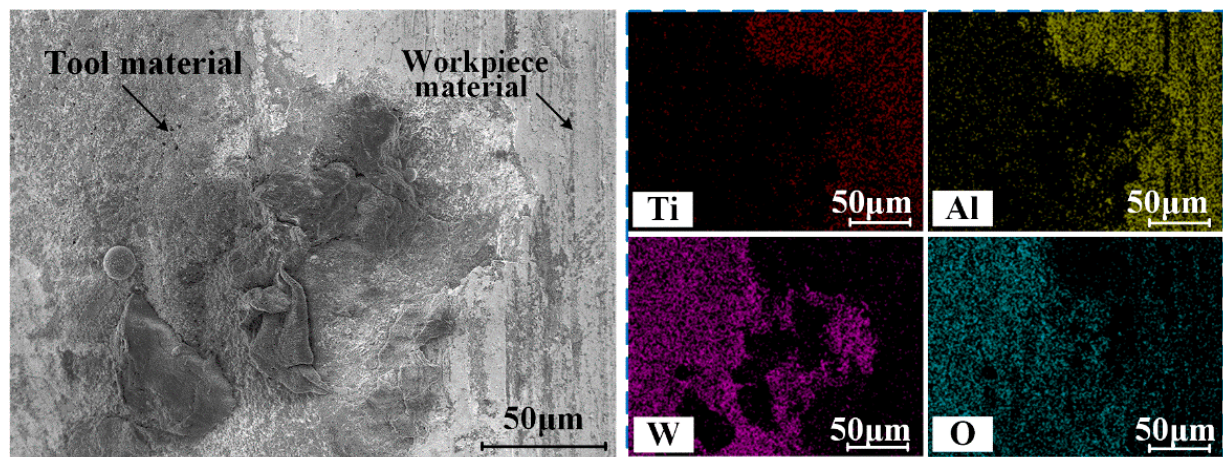


Figure 9. The morphology and EDS analysis of region A in Figure 6b.

Table 4. The Element composition of region 4/5/6.

Cutting Speed	Element Composition (at%)							
	Ti	Al	V	Cr	W	C	Co	O
60	30.23	34.31	1.67	1.44	0.04	32.31	-	-
120	17.79	30.97	0.98	1.40	0.21	32.52	0.13	15.99
180	19.51	23.63	0.80	0.57	0.31	34.87	0.50	19.81

**Figure 10.** The morphology and EDS analysis of region B in Figure 7b.**Table 5.** The Element composition of region 7/8/9.

Cutting Speed	Element Composition (at%)							
	Ti	Al	V	Cr	W	C	Co	O
60	21.78	29.92	0.83	0.21	0.03	47.23	-	-
120	14.53	24.83	0.76	0.94	0.35	46.95	0.12	11.51
180	14.32	22.35	0.73	0.78	0.51	45.43	0.80	15.08

Cutting speed has a major influence on the wear mechanism of the tool. As the cutting speed increases, the surface of the tool will be affected by factors such as higher temperature, stress, and pressure, which will easily cause thermal fatigue, structural changes, plastic deformation, and adhesive wear. Cutting forces are also critical to the wear mechanism of the tool. When cutting γ -TiAl alloy at high speed at low temperatures, the cutting force is large, which will cause plastic deformation and scratches on the surface of the tool. These deformations will gradually intensify, leading to early failure of the tool. There is currently no evidence that cutting speed and cutting force affect tool wear mechanisms significantly differently. Therefore, in the actual cutting process, it is necessary to balance the cutting speed and cutting force to ensure the life of the tool and the processing quality of the workpiece.

3.4. Surface Roughness

To further study the feasibility of cryogenic conditions in γ -TiAl alloy machining, the machined surfaces under various cutting conditions are analyzed. The average surface roughness (R_a) of the workpiece is obtained, as shown in Figure 11. The R_a measured under the other two cooling conditions is significantly lower than that under dry conditions.

When the cutting speed is 60 m/min, the R_a obtained by the emulsion condition is lower than that obtained by the LN_2 condition because good lubrication of emulsion makes it easier to get a smooth surface at low speeds. The material in the cutting layer is cooled rapidly in LN_2 condition, which reduces the thermal softening effect. Moreover, γ -TiAl

alloy has high brittleness in a cryogenic environment. The machined surface with poor quality is obtained during low-speed cryogenic machining. When the cutting speed is increased, the cutting vibration and high cutting temperature brought by the high speeds increase the instability, aggravating the tool wear. In addition, severe work-hardening and higher cutting force increase the machining difficulty. It is not conducive to the formation of a machined surface with high quality. Therefore, when $v_c = 120$ m/min in dry machining, the R_a value reaches the peak value. The emulsion and LN_2 environment has a positive effect on reducing tool wear; the R_a reaches the peak value at $v_c = 150$ m/min. When the cutting speed is higher than the critical speeds, the thermal softening effect of the material is significant. The lower surface roughness is produced by the plowing effect.

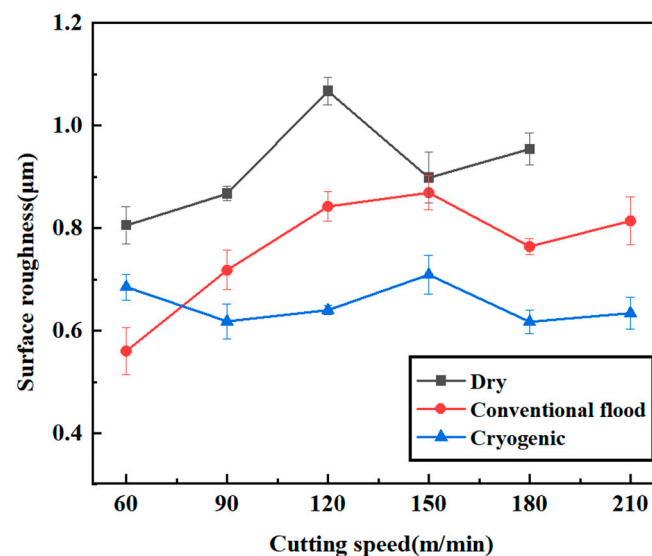


Figure 11. The surface roughness under various cutting conditions.

With the further increase of cutting speed, the tool cutting edge deteriorates under the action of mechanical and thermal load. As a result, the R_a value increases. Compared with the other two conditions, the variation degree of R_a under the LN_2 condition is the smallest in the selected cutting speed range.

Cutting in the cryogenic coolant can effectively reduce tool wear, and cutting with sharp tools can obtain a more ideal machined surface. Cryogenic cooling reduces the plasticity of the material and reduces the side flow of the material during the cutting process, which also makes the machined surface close to the ideal morphology.

3.5. Microstructure Morphology of Sub-Surface

To further explore the influence of cooling conditions on the machined surface, the microstructure of the cross-section of the workpiece is observed, as shown in Figure 12. The microstructure of the sub-surface has changed, which is mainly reflected by lamellar deformation. Obvious lamellar deformation occurs under dry and conventional flood cooling conditions. The plastic deformation will lead to residual tensile stress, which will affect the fatigue resistance of the workpiece [41]. A cryogenic cooling environment weakens the influence of the thermal effect, resulting in the reduction of microstructure deformation.

In addition, some grain boundaries protrude into adjacent grains at about $10\ \mu\text{m}$ below the surface layer compared with the original obvious vertical grain boundary of the workpiece. The grain boundary is fuzzy. The reason is that some grain boundaries bend under thermal activation, and the mobility of grain boundaries is improved. The two adjacent lamellas erode each other, resulting in the blurring of the boundary between the tissues. When the cutting temperature reaches a certain degree, the $\gamma + \alpha_2$ lamellar microstructure is broken. The dynamic recrystallization of the γ and the spheroidization of the α_2 occur, which can refine the grain structure. Some studies [42–44] show that the

temperature range of γ and α_2 change is the brittle–ductile transition range of γ -TiAl alloy. The transition in γ -TiAl alloy cutting from brittleness removal to plasticity removal proves the possibility of turning points in the V_{max} , F , and Ra in the above analysis. Beretta et al. [45] proposed that the fully lamellar microstructure induces higher strain localizations in a single lamellar grain, and the presence of equiaxed grains at the lamellar grain boundaries can be beneficial in limiting the high local strains, which is similar to the conclusions of this study.

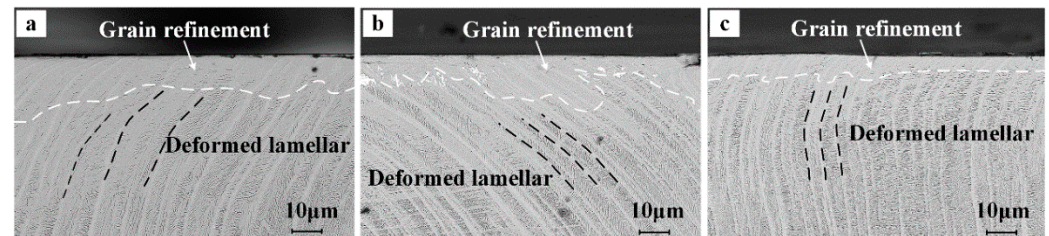


Figure 12. The microstructure morphology under various cutting conditions at $v_c = 120$ m/min (a) dry; (b) conventional flood cooling; (c) cryogenic cooling.

4. Conclusions

To suppress tool wear and improve surface quality, the feasibility of cryogenic cooling in γ -TiAl alloy high-speed cutting was explored. This paper studied the tool wear and mechanism, cutting force, as well as surface and sub-surface morphology characteristics under various cooling media and cutting speeds. The conclusions are as follows.

- (a) The flank and rake face of the tool are worn to varying degrees at high-speed turning. The crater wear is observed on the rake face at $v_c = 60$ m/min. With the increase in cutting speed, the crater wear is expanded, progressing into more severe flaking and notching wear. LN_2 -assisted cutting delays the occurrence of this state and greatly improves the tool life;
- (b) The main wear pattern in dry machining is gradually transformed from adhesive wear to diffusion and oxidation wear at high speeds. The wear mechanism is still mainly adhesive wear in emulsion and LN_2 cooling conditions, accompanied by slight diffusion and oxidation wear. Cryogenic cooling has a significant effect on inhibiting adhesion, diffusion, and oxidative wear;
- (c) Cryogenic cooling-assisted high-speed machining can significantly improve the surface finish and inhibit the deformation of the sub-surface microstructure. To some extent, the cooling effect of LN_2 inhibits thermal activation and reduces the degree of grain refinement. However, the combination of cryogenic cooling and high-speed machining technology is a field worthy of exploration from a long-term perspective;
- (d) The curves of the V_{max} , F , and Ra turn at $v_c = 120$ m/min in dry conditions and at $v_c = 150$ m/min in emulsion and LN_2 conditions. It is preliminarily considered that the brittle–ductile transition of γ -TiAl alloy occurs within this cutting speed range. Further exploration is needed in future research work.

5. Prospect

Despite its numerous advantages, there are some potential drawbacks to the use of LN_2 cryogenic cooling. One of the main challenges is the cost associated with the storage and transportation of LN_2 , and the other is that for some materials, LN_2 is excessively cold, and extremely low temperature is harmful to the surface integrity on the contrary.

For the first issue, the consumption of LN_2 should be optimized, so subsequent research on minimal-cryogenic cooling is needed. For the second issue, some other cryogenic medium may be a suitable alternative, such as LCO_2 , which could provide a more moderate cryogenic condition. Therefore, various factors such as workpiece material, cutting conditions, and production costs should be considered when selecting cryogenic cooling process parameters in the future.

Author Contributions: Conceptualization, X.W.; data curation, D.P.; funding acquisition, X.W., X.F. and Y.Q.; investigation, D.P.; methodology, X.W. and D.P.; supervision, X.W., X.F. and Y.Q.; validation, D.P.; writing—original draft, X.W., X.Z. and D.P.; writing—review and editing, X.W., X.Z., J.N. and X.F. All authors have read and agreed to the published version of the manuscript.

Funding: This work was funded by the National Natural Science Foundation of China (Grant No. 52005215 and 52175408) and the Project of Shandong Province Higher Educational Science and Technology Program (Grant No. 2019KJB021), and the APC was funded by the National Natural Science Foundation of China (Grant No. 52005215).

Conflicts of Interest: The authors declare that they have no known competing financial interest or personal relationships that could have appeared to influence the work reported in this paper. Author Duo Pan was employed by the company Jigang International Engineering & Technology Co., Ltd. The remaining authors declare that the research was conducted in the absence of any commercial or financial relationships that could be construed as a potential conflict of interest.

References

1. Xu, R.; Li, M.; Zhao, Y. A review of microstructure control and mechanical performance optimization of γ -TiAl alloys. *J. Alloys Compd.* **2022**, *932*, 167611. [\[CrossRef\]](#)
2. Castellanos, S.; Cavaleiro, A.J.; Jesus, A.D.; Neto, R.; Alves, J.L. Machinability of titanium aluminides: A review. *Materials* **2019**, *233*, 426–451. [\[CrossRef\]](#)
3. Clemens, H.; Mayer, S. Design, processing, microstructure, properties, and applications of advanced intermetallic TiAl alloys. *Adv. Eng. Mater.* **2013**, *15*, 191–215. [\[CrossRef\]](#)
4. Hood, R.; Aspinwall, D.K.; Voice, W. Creep feed grinding of γ -TiAl using single layer electroplated diamond super abrasive wheels. *CIRP J. Manuf. Sci. Technol.* **2015**, *11*, 36–44. [\[CrossRef\]](#)
5. Yao, C.F.; Lin, J.N.; Wu, D.X.; Junxue, R.E. Surface integrity and fatigue behavior when turning γ -TiAl alloy with optimized PVD-coated carbide inserts. *Chin. J. Aeronaut.* **2018**, *145*, 214–224. [\[CrossRef\]](#)
6. Priarone, P.C.; Robiglio, M.; Settineri, L.; Tebaldo, V. Milling and Turning of Titanium Aluminides by Using Minimum Quantity Lubrication. *Procedia CIRP* **2014**, *24*, 62–67. [\[CrossRef\]](#)
7. Beranoagirre, A.; López de Lacalle, L.N. Optimizing the turning of titanium aluminide alloys. *Adv. Mater. Res.* **2012**, *498*, 189–194. [\[CrossRef\]](#)
8. Beranoagirre, A.; López de Lacalle, L.N. Optimising the milling of titanium aluminide alloys. *Int. J. Mechatron. Manuf. Syst.* **2010**, *3*, 425–436. [\[CrossRef\]](#)
9. Beranoagirre, A.; de Lacalle, L.N.L. Grinding of gamma TiAl intermetallic alloys. *Procedia Eng.* **2013**, *63*, 489–498. [\[CrossRef\]](#)
10. Cheng, Y.; Yuan, Q.; Zhang, B.; Wang, Z. Study on turning force of γ -TiAl alloy. *Int. J. Adv. Manuf. Technol.* **2019**, *105*, 2393–2402. [\[CrossRef\]](#)
11. Beranoagirre, A.; Olvera, D.; López de Lacalle, L.N. Milling of gamma titanium–aluminum alloys. *Int. J. Adv. Manuf. Technol.* **2012**, *62*, 83–88. [\[CrossRef\]](#)
12. Wang, B.; Liu, Z.Q.; Su, G.S.; Song, Q.; Ai, X. Investigations of critical cutting speed and ductile-to-brittle transition mechanism for workpiece material in ultra-high speed machining. *Int. J. Mech. Sci.* **2015**, *104*, 44–59. [\[CrossRef\]](#)
13. Aspinwall, D.K.; Mantle, A.L.; Chan, W.K.; Hood, R.; Soo, S.L. Cutting temperatures when ball nose end milling γ -TiAl intermetallic alloys. *CIRP Ann.-Manuf. Technol.* **2013**, *62*, 75–78. [\[CrossRef\]](#)
14. Klocke, F.; Lung, D.; Arft, M.; Priarone, P.C.; Settineri, L. On high-speed turning of a third-generation gamma titanium aluminide. *Int. J. Adv. Manuf. Technol.* **2013**, *65*, 155–163. [\[CrossRef\]](#)
15. Saketi, S.; Odelros, S.; Östby, J.; Olsson, M. Experimental Study of Wear Mechanisms of Cemented Carbide in the Turning of Ti6Al4V. *Materials* **2019**, *12*, 2822. [\[CrossRef\]](#) [\[PubMed\]](#)
16. Rajashree, M.; Ramanuj, K.; Amlana, P.; Kumar, S.A. Current Status of Hard Turning in Manufacturing: Aspects of Cooling Strategy and Sustainability. *Lubricants* **2023**, *11*, 108.
17. Zou, L.; Huang, Y.; Zhang, G.J.; Cui, X. Feasibility study of a flexible grinding method for precision machining of the TiAl-based alloy. *Mater. Manuf. Process.* **2019**, *34*, 1160–1168. [\[CrossRef\]](#)
18. Wang, Z.H.; Liu, Y.W. Study of surface integrity of milled gamma titanium aluminide. *J. Manuf. Process.* **2020**, *56*, 806–819. [\[CrossRef\]](#)
19. Ezugwu, E.O. High speed machining of aero-engine alloys. *J. Braz. Soc. Mech. Sci. Eng.* **2004**, *26*, 1–11. [\[CrossRef\]](#)
20. Liu, Z.; An, Q.; Xu, J.; Chen, M.; Han, S. Wear performance of (nc-AlTiN)/(a-Si₃N₄) coating and (nc-AlCrN)/(a-Si₃N₄) coating in high-speed machining of titanium alloys under dry and minimum quantity lubrication (MQL) conditions. *Wear* **2013**, *305*, 249–259. [\[CrossRef\]](#)
21. Klocke, F.; Settineri, L.; Lung, D.; Claudio Priarone, P.; Arft, M. High performance cutting of gamma titanium aluminides: Influence of lubricoolant strategy on tool wear and surface integrity. *Wear* **2013**, *302*, 1136–1144. [\[CrossRef\]](#)
22. González, H.; Pereira, O.; López de Lacalle, L.N.; Calleja, A.; Ayesta, I.; Muñoa, J. Flank-milling of integral blade rotors made in Ti₆Al₄V using Cryo CO₂ and minimum quantity lubrication. *J. Manuf. Sci. Eng.* **2021**, *143*, 091011. [\[CrossRef\]](#)

23. Khanna, N.; Shah, P.; de Lacalle, L.N.L.; Rodríguez, A.; Pereira, O. In pursuit of sustainable cutting fluid strategy for machining Ti-6Al-4V using life cycle analysis. *Sustain. Mater. Technol.* **2021**, *29*, e00301. [[CrossRef](#)]
24. M'Saoubi, R.; Axinte, D.; Soo, S.L.; Nobel, C.; Attia, H.; Kappmeyer, G.; Engin, S.; Sim, W.-M. High performance cutting of advanced aerospace alloys and composite materials. *CIRP Ann.-Manuf. Technol.* **2015**, *64*, 557–580. [[CrossRef](#)]
25. Devaraya, R.G.; Raviraj, S.; Rao, S.S.; Gaitonde, V.N. Analysis of Surface Roughness and Hardness in Titanium Alloy Machining with Polycrystalline Diamond Tool under Different Lubricating Modes. *Mater. Res.* **2014**, *17*, 1010–1022.
26. Jawahir, I.S.; Attia, H.; Biermann, D.; Duflou, J.; Klocke, F.; Meyer, D.; Newman, S.T.; Pusavec, F.; Putz, M.; Rech, J.; et al. Cryogenic manufacturing processes. *CIRP Ann.-Manuf. Technol.* **2016**, *65*, 713–736. [[CrossRef](#)]
27. Pratham, S.; Rohit, N.; Ramanuj, K.; Deepak, S.; Amlana, P.; Kumar, S.A.; Diptikanta, D. Cryogenics as a Cleaner Cooling Strategy for Machining Applications: A Concise Review. *Int. J. Energy A Clean Environ.* **2022**, *23*, 129–141.
28. Navneet, K.; Chetan, A.; Yu, P.D.; Kumar, S.A.; Rocha, M.A.; Ribeiro, S.L.R.; Kumar, G.M.; Murat, S.; Grzegorz, M.K. Review on design and development of cryogenic machining setups for heat resistant alloys and composites. *J. Manuf. Process.* **2021**, *68*, 398–422.
29. Shah, P.; Khanna, N.; Chetan. Comprehensive Machining Analysis to Establish Cryogenic LN₂ and LCO₂ as Sustainable Cooling and Lubrication Techniques. *Tribol. Int.* **2020**, *148*, 106314. [[CrossRef](#)]
30. Musfirah, A.H.; Ghani, J.A.; Haron, C. Tool wear and surface integrity of Inconel 718 in dry and cryogenic coolant at high cutting speed. *Wear* **2017**, *376–377*, 125–133. [[CrossRef](#)]
31. Yildirim, C.V. Experimental comparison of the performance of nanofluids, cryogenic and hybrid cooling in turning of Inconel 625. *Tribol. Int.* **2019**, *137*, 366–378. [[CrossRef](#)]
32. Shokrani, A.; Dhokia, V.; Newman, S.T. Investigation of the effects of cryogenic machining on surface integrity in CNC end milling of Ti-6Al-4V titanium alloy. *J. Manuf. Process.* **2016**, *21*, 172–179. [[CrossRef](#)]
33. Sartori, S.; Ghiotti, A.; Bruschi, S. Hybrid lubricating/cooling strategies to reduce the tool wear in finishing turning of difficult-to-cut alloys. *Wear* **2017**, *376–377*, 107–114. [[CrossRef](#)]
34. Zhao, W.; Ren, F.; Iqbal, A.; Gong, L.; He, N.; Xu, Q. Effect of liquid nitrogen cooling on surface integrity in cryogenic milling of Ti-6Al-4V titanium alloy. *Int. J. Adv. Manuf. Technol.* **2020**, *106*, 1497–1508. [[CrossRef](#)]
35. Fernández, D.; Sandá, A.; Bengoetxea, I. Cryogenic Milling: Study of the Effect of CO₂ Cooling on Tool Wear When Machining Inconel 718, Grade EA1N Steel and Gamma TiAl. *Lubricants* **2019**, *7*, 10. [[CrossRef](#)]
36. Pereira, O.; Urbikain, G.; Rodríguez, A.; Fernández-Valdivielso, A.; Calleja, A.; Ayesta, I.; de Lacalle, L.L. Internal cryo lubrication approach for Inconel 718 milling. *Procedia Manuf.* **2017**, *13*, 89–93. [[CrossRef](#)]
37. Priarone, P.C.; Klocke, F.; Faga, M.G.; Lung, D.; Settineri, L. Tool life and surface integrity when turning titanium aluminides with PCD tools under conventional wet cutting and cryogenic cooling. *Int. J. Adv. Manuf. Technol.* **2016**, *85*, 807–816. [[CrossRef](#)]
38. Yuan, Q.; Cheng, Y.; Wang, Z.H.; Hu, X. Failure study of carbide tools for turning γ -TiAl alloys. *Tool Eng.* **2019**, *53*, 12–16.
39. Astakhov, V. *Tribology of Metal Cutting*; Elsevier: Amsterdam, The Netherlands, 2006.
40. Jiang, Z.H.; Wang, L.L.; Shi, L. Study on Tool Wear Mechanism and Characteristics of Carbide Tools in Cutting Ti6Al4V. *J. Mech. Eng.* **2014**, *50*, 178–184. [[CrossRef](#)]
41. Tian, S.; Qi, W.; Yu, H.; Sun, H.; Li, Q. Microstructure and creep behaviors of a high Nb-TiAl intermetallic compound based alloy. *Mater. Sci. Eng. A* **2014**, *614*, 338–346. [[CrossRef](#)]
42. Wang, Q.; Chen, R.; Gong, X.; Guo, J.; Su, Y.; Ding, H.; Fu, H. Microstructure, Mechanical Properties, and Crack Propagation Behavior in High-Nb TiAl Alloys by Directional Solidification. *Metall. Mater. Trans. A* **2018**, *49*, 4555–4564. [[CrossRef](#)]
43. Wang, Q.; Chen, R.; Chen, D.; Su, Y.; Ding, H.; Guo, J.; Fu, H. The characteristics and mechanisms of creep brittle-ductile transition in TiAl alloys. *Mater. Sci. Eng.* **2019**, *767*, 138393. [[CrossRef](#)]
44. Wei, W.; Zeng, W.; Chen, X.; Liang, X.; Zhang, J. Microstructural evolution, creep, and tensile behavior of a Ti-22Al-25Nb (at%) orthorhombic alloy. *Mater. Sci. Eng. A* **2014**, *603*, 176–184.
45. Patriarca, L.; Içöz, C.; Filippini, M.; Beretta, S. Microscopic Analysis of Fatigue Damage Accumulation in TiAl Intermetallics. *Key Eng. Mater.* **2014**, *592–593*, 30–35.

Disclaimer/Publisher's Note: The statements, opinions and data contained in all publications are solely those of the individual author(s) and contributor(s) and not of MDPI and/or the editor(s). MDPI and/or the editor(s) disclaim responsibility for any injury to people or property resulting from any ideas, methods, instructions or products referred to in the content.